Journal of Materials Chemistry A

Accepted Manuscript

ROYAL SOCIETY OF CHEMISTRY

www.rsc.org/materialsA

Journal of Materials Chemistry A RSCPublishing

COMMUNICATION

$Pr_2O_2SO_4$- $La_{0.6}Sr_{0.4}Co_{0.2}Fe_{0.8}O_{3-\delta}$: a new category of composite cathode for Intermediate Temperature-Solid Oxide Fuel Cells

Cite this: DOI: 10.1039/x0xx00000x

Received ooth January 2012,
Accepted ooth January 2012

DOI: 10.1039/x0xx00000x

www.rsc.org/

Francisco J. A. Loureiro,[a] Tao Yang[a], Daniel G. Stroppa[b], and Duncan P. Fagg[a]*

A new category of composite cathode for solid oxide fuel cells is investigated, containing an oxysulphate oxygen storage material. A stable composite $Pr_2O_2SO_4$-$La_{0.6}Sr_{0.4}Co_{0.2}Fe_{0.8}O_{3-\delta}$ is formed, providing significant improvements in the total polarization resistance, predominantly due to improvements in the processes of interfacial charge transfer and surface exchange.

Solid Oxide Fuel Cells (SOFCs) can efficiently convert chemical energy directly into electricity, by oxidation of fuels such as H_2 or even hydrocarbons, with minimum pollution and silently.[1] High-temperature fuel cells (HTFCs), targeted at working temperatures around 800-1000 °C, are promising devices due to their flexibility to a wide diversity and purity of fuels and the possibility to use affordable catalysts.[2] Nonetheless, current works promote a slight decrease in operation temperature, to the intermediate-temperature range (600-800 °C), to improve longevity and to make the overall SOFC technology more affordable.[3,4] On the other hand, a drawback to working at lower temperatures is an associated increase in the area specific resistance, as a consequence of increased polarization resistance (R_p) and lowered electrolyte conductivity.[5] To minimize cathode polarization losses, the choice of an appropriate electrode composition and microstructure, thus, become critical factors at intermediate temperatures to maximize the kinetics of oxygen exchange and diffusion.[5]

State of the art SOFC cathodes are composite materials consisting of $(ZrO_2)_{0.92}(Y_2O_3)_{0.08}$, YSZ, a classical ionic conductor, and $La_{1-x}Sr_xMnO_{3-\delta}$, LSM, an electronic conductor.[5] Although the pure LSM phase performs adequately at 1000 °C, its poor oxide ionic transport hinders electrode kinetics at lower temperatures, thereby, necessitating combination with YSZ to retain acceptable electrochemical performance.[6] Single phase mixed ionic and electronic conducting (MIECs) materials have also been suggested as potential cathodes, such as $La_{0.6}Sr_{0.4}Co_{0.8}Fe_{0.2}O_{3-\delta}$ (LSCF), $Sm_{0.5}Sr_{0.5}Co_{0.5}O_{3-\delta}$ (SSC), and $Ba_{0.5}Sr_{0.5}Co_{0.2}Fe_{0.8}O_{3-\delta}$ (BSCF).[7] Of these, LSCF is the most widely used, due to its low cost and good performance,[4,5,8] offering high electronic (230 S cm^{-1} at 900 °C) and ionic conductivities (0.2 S cm^{-1} at 900 °C).[6]

Mirroring the composite concept of YSZ-LSM, several pure ionic conductors have been combined with LSCF to make a composite cathode, such as $(ZrO_2)_x(Sc_2O_3)_{1-x}$ (ScSZ), $La_{1-x}Sr_xGa_{1-y}Mg_yO_{3-(x+y)/2}$ (LSGM) or $(CeO_2)_{1-x}(GdO_{1.5})_x$ (CGO). These materials offer the advantage of superior ionic conductivity at intermediate temperatures (by up to an order of magnitude) in comparison to that of YSZ. Nevertheless, the chemical instability of LSGM[9] and the reported interaction of LSCF with ScSZ, to form Strontium Zirconate ($SrZrO_3$) and Lanthanum Zirconate ($La_2Zr_2O_7$), as well as high cost make these solutions problematic.[10] Against this background, there are clear advantages for the use of CGO as the secondary cathode component, regarding its good chemical compatibility, price and high ionic conductivity. Thus, several works can be found in literature concerning the electrochemical behavior of the composite cathode material, LSCF-CGO. Murray et al.[6] assessed the electrode performance of different fractions of CGO in the LSCF-CGO composite, showing the composition LSCF-CGO (50 wt% of CGO) to offer the lowest R_p value of 0.33 Ω cm^2, at 600 °C in air. In contrast, the work of Dusastre et al.[11] placed peak performance at a CGO content of 30 wt% with an improvement of 4 times in R_p over that of the pure LSCF phase. Dusastre et al. further outlined that the compositional dependence of peak performance is intricately linked to the electrode microstructure, with the CGO/LSCF ratio needed for peak electrochemical performance, increasing with decreasing porosity.[11]

The main processes suggested to dominate the kinetics of mixed conducting SOFC cathodes are that of diffusion of ionic species through the bulk of the electrode and surface exchange reactions, such as charge transfer and dissociative adsorption of oxygen on the electrode surface[12,13] These principal phenomena may also be accompanied by additional resistive terms corresponding to electrochemical kinetic limitations at the electrode/electrolyte interface and/or gas phase limitations.[12,13] For the principal processes, Liu[13] described how the resistance to solid state mass transport though the mixed conducting electrode path could be related to the sum of the ionic and electronic resistivities, combined with that of surface exchange. Liu also highlighted that both of these factors are commonly related to the level of ambipolar conductivity in MIEC materials.[12,14–16] Correspondingly, authors have shown how maximization of the ambipolar conductivity, by the formation of composite electrodes such as LSCF-CGO, can offer peak performing cathodes of low polarization resistances.[11] Here the presence of the CGO phase becomes increasingly important to retain electrochemical performance at lower temperatures, due to limitations of ionic transport in LSCF as a result of its higher activation energy for ionic migration than that of CGO.[11]

In an unconventional departure from previous materials, the current study offers a completely new category of composite cathode for SOFCs based on combination of LSFC with the material $Pr_2O_2SO_4$. Ln oxysulfate materials (Ln = La, Pr, Nd and Sm) possess high surface area and uniform mesoporosity, and have been considered as candidates for oxygen storage due to the redox ability of sulfur.[17,18] Among Ln-based oxysulfates, the Pr system has the lowest possible operational temperature (around 600 °C), where the additional redox couple between Pr^{3+} and Pr^{4+} at the surface promotes the redox of sulfur, facilitating Pr_2O_2S formation.[19] The transport properties of $Pr_2O_2SO_4$ are currently unknown. However, the availability of rapid oxygen exchange can be considered a potentially useful property for incorporation in a SOFC cathode, due to the aforementioned primary cathode limitations of charge transfer and dissociative adsorption of oxygen on the electrode surface. Therefore, the potential of $Pr_2O_2SO_4$ as the secondary component in a SOFC cathode is investigated in the current work. A $Pr_2O_2SO_4$-LSCF composite in a 50vol% ratio is carefully characterized in terms of chemical compatibility, microstructure and electrokinetic behavior and is shown to offer valuable performance gains over that of a pure LSCF cathode.

Fig. 1 shows the XRD pattern of $Pr_2O_2SO_4$-LSCF powder after heat treatment at 1100 °C, during 24 h.

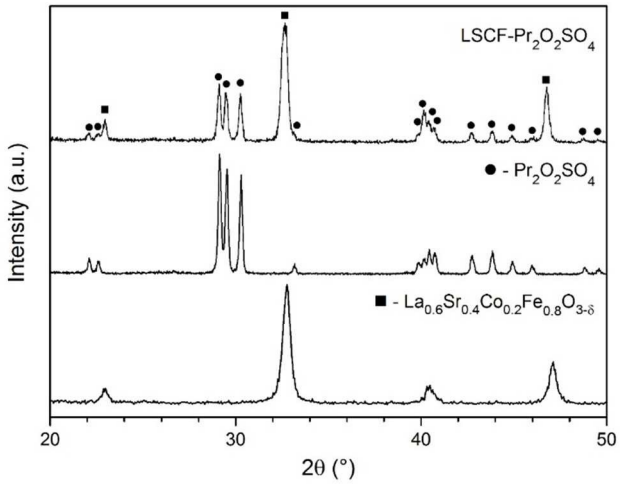

Fig. 1 – XRD pattern of $La_{0.6}Sr_{0.4}Co_{0.2}Fe_{0.8}O_{3-\delta}$-$Pr_2O_2SO_4$ composite after heat treatment at 1100 °C, during 24 h.

Only two phases were identified: $La_{0.6}Sr_{0.4}Co_{0.2}Fe_{0.8}O_{3-\delta}$ with a rhombohedral (trigonal) structure in the $R\bar{3}$ c space group (No. 167) and $Pr_2O_2SO_4$ with a monoclinic structure with the C2/c (No. 15) space group. No extra peaks or notable peak shifts were observed, indicating the apparent absence of chemical interreaction between LSCF and $Pr_2O_2SO_4$ under these conditions.

Fig. 2 a) and b) present the top view microstructures of pure LSCF and the $Pr_2O_2SO_4$-LSCF composite, respectively, showing similar microstructures. Fig. 2 c) shows an example three-dimensional reconstruction of the pores of a cathode film retrieved by a "slice and view" approach using a combined Focused Ion Beam (FIB) - Scanning Electron Microscope (SEM) technique. By this approach, the electrode structures are shown to be approximately 2 µm in thickness and to offer interconnecting pores, with similar porosity levels of 14% and 18% for the LSCF and $Pr_2O_2SO_4$-LSCF cathode films, respectively. Fig. 2 d) shows a qualitative composition map of the composite film by SEM-XEDS, which indicates an intimate distribution of the LSCF and $Pr_2O_2SO_4$ phases and their chemical independence.

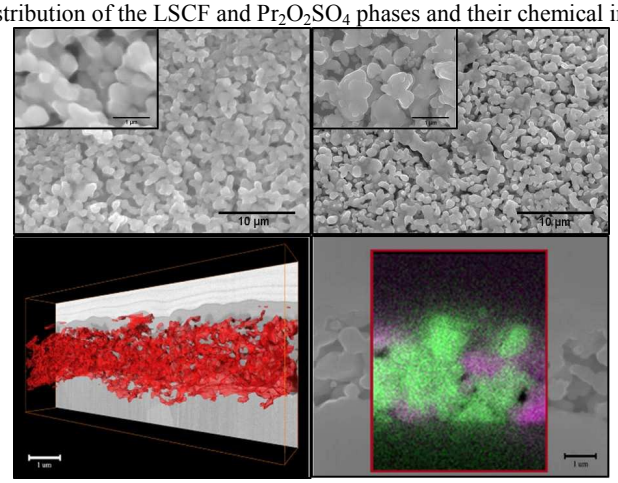

Fig. 2 – Cross-section SEM images (SE) from the a) LCSF film and the b) composite film; c) perspective view of the reconstructed pores structure (red) from the LCSF film; d) qualitative composition map from the composite film by SEM-XEDS. The green color refers to La-Lα signal, while the purple color refers to a sum of Pr-Lα and S-Kα signals. The scale bar in the insets of figures c) and d) indicates 1 µm.

The impedance spectra of obtained for symmetrical cathode/electrolyte/cathode cells correspond to partially overlapped, depressed arcs for both the pure LSCF and the $Pr_2O_2SO_4$-LSCF cathodes. The impedance responses were modelled by an equivalent circuit, previously suggested in the literature for LSCF[20], consisting of a resistor, R_1, representing the ohmic resistance, in series with a combination of a Warburg element and several parallel R||CPE elements, Fig. 3, that together describe the overall electrode polarisation resistance, R_p. For the R||CPE elements, R is a resistance (Ω) and CPE is a constant phase element, defined as $\boldsymbol{Z_{CPE} = Q_i^{-1}(i\omega)^{-n}}$; ω is the angular frequency and Q_i and n are the usual parameters characterizing the pseudo-capacitance and the phase angle, respectively. Previous works show that these parameters can provide information on the elementary cathodic reaction steps,[17,21,20] each of which is described by a specific relaxation frequency, ω_0, given by $\boldsymbol{\omega_0 = (RC)^{-1}}$, of effective capacitance $\boldsymbol{C = R^{1/n-1}Q^{1/n}}$. In the case of the $Pr_2O_2SO_4$-LSCF composite an additional R||CPE element was also found to be necessary at low temperatures to accommodate a further low frequency response (R_5||CPE_5).

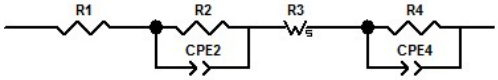

Fig. 3 – Equivalent electric circuit used in modelling experimental impedance diagrams.[20]

In terms of global behavior, the total electrode polarization resistance, $R_p = R_2 + R_3 + R_4 + R_5$, is shown to be significantly lower in the composite material. For example, $R_p = 1.75\ \Omega\ cm^2$ for LSCF at 771°C in oxygen, while a value 5 times lower than this is offered in the case of the composite, $0.35\ \Omega\ cm^2$, Fig.4. The activation energy (E_a) values of the total electrode polarization resistance, corresponds to 1.76 and 1.90 eV for the composite and LSCF, respectively. The R_p and E_a values obtained for LSCF in the current work are at the high end of those previously reported for this cathode.[22,23] Nonetheless, the performance of LSCF has been documented to be sensitive to processing conditions, such as sintering temperature, [24] and the current work provides a comparison of cathode materials of similar microstructures formed under similar processing conditions.

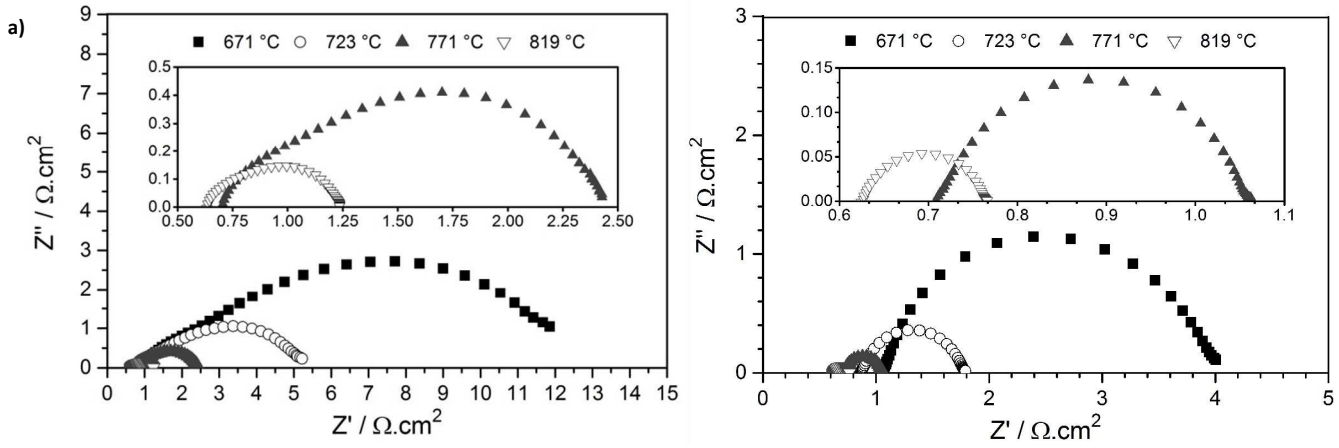

Fig. 4 – Impedance spectra of a) LSCF|CGO and b) LSCF-$Pr_2O_2SO_4$|CGO symmetric cells, measured at pO_2 = 1 atm.

The oxygen partial pressure dependencies of the polarization resistances are shown in Fig. 5. From these results, it is possible to observe that R_p decreases with increasing pO_2.

For both LSCF and the composite, the high frequency arc, corresponding to polarization resistance R_2, shows negligible pO_2 dependence, suggesting neither atomic oxygen or molecular oxygen is involved in the process.[20,25] Such an analogy would correspond to previous literature of LSCF which suggest the high frequency response to be related to the presence of interfacial charge-transfer processes,[12,13,20] although the exact nature of this feature remains an open question.[26] In pure oxygen, the corresponding capacitance values of this response are in the order of 10^{-5} F cm^{-2} for both LSCF and composite, further concurring with typical values reported for this contribution.[12,13,20]

Concerning the intermediate frequency responses, corresponding to the polarization resistances R_3 and R_4, a Warburg element was used to simulate the response of R_3, to represent bulk ionic diffusion.[20] The pO_2^n dependence of this resistance term was shown to range from 0.11 to 0.17 for the composite and from 0.06 to 0.15 for LSCF, Fig. 5, in agreement with that previously reported for LSCF.[20] Regarding the capacitance of this term, values in the range of 10^{-3}-10^{-4} F cm^{-2}, in pure oxygen, were determined for both materials. In contrast, R_4 presents a pO_2^n dependence ranging from 0.28 to 0.31 for LSCF and from 0.25 to 0.28 for the composite, Fig. 5, values which are indicative that surface exchange is rate determining (n = 0.25).[20,21] The capacitance of this term exhibits values in the order of 10^{-2} F cm^{-2} in both cases, again agreeing with that reported for LSCF.[20,21] The corresponding activation energy values, E_a, are calculated as 1.84 and 1.92 eV for LSCF and the composite, respectively, in oxygen; values that are slightly higher than those previously documented for this term (1.1-1.6 eV).[20,21] Both R_3 and R_4 presents relatively high capacitance values that can be considered typical for the chemical capacitance arising from changes of oxygen stoichiometry within the electrode.[11,25,26]

The low frequency response, R_5, observable only in the composite material and at low temperatures, presents the highest pO_2 dependence, with n ~0.5, possibly implying a dissociative adsorption mechanism.[21,26,27]

Bringing together the effects of temperature and oxygen partial pressure and the microstructural analysis, we will now summarize the main relevant aspects. The polarization resistances R_2 and R_4 are by far the most affected polarization responses by the addition of $Pr_2O_2SO_4$, especially for lower temperatures. For example, at 771 °C, R_2 experiences a decrease from 0.13 to 0.01 $\Omega\ cm^2$, respectively for LSCF and composite, which is remarkably 15 times lower; while R_4, decreases by 6 times from 1.47 to 0.26 $\Omega\ cm^{-2}$. In contrast, R_3 is only reduced from 0.15 to 0.04 $\Omega\ cm^2$, 4 times lower, at this temperature, while R_4 reduces from 0.59 to 0.26 $\Omega\ cm^2$. These improvements lead to an overall gain in performance for the composite material with respect to pure LSCF.[11] As simple microstructural effects can be discarded, since both cathode materials of the current study show similar levels of porosity and thickness, discussion should be based on the possible intrinsic properties of $Pr_2O_2SO_4$ that could lead to such improvements.[12,20,21] In oxidizing conditions, $Pr_2O_2SO_4$ is composed of alternative stacks of $Pr_2O_2^{2+}$ and SO_4^{2-} units (Fig. 6), while upon reduction, sulphur is reduced, with loss of oxygen from the sulphate layers.

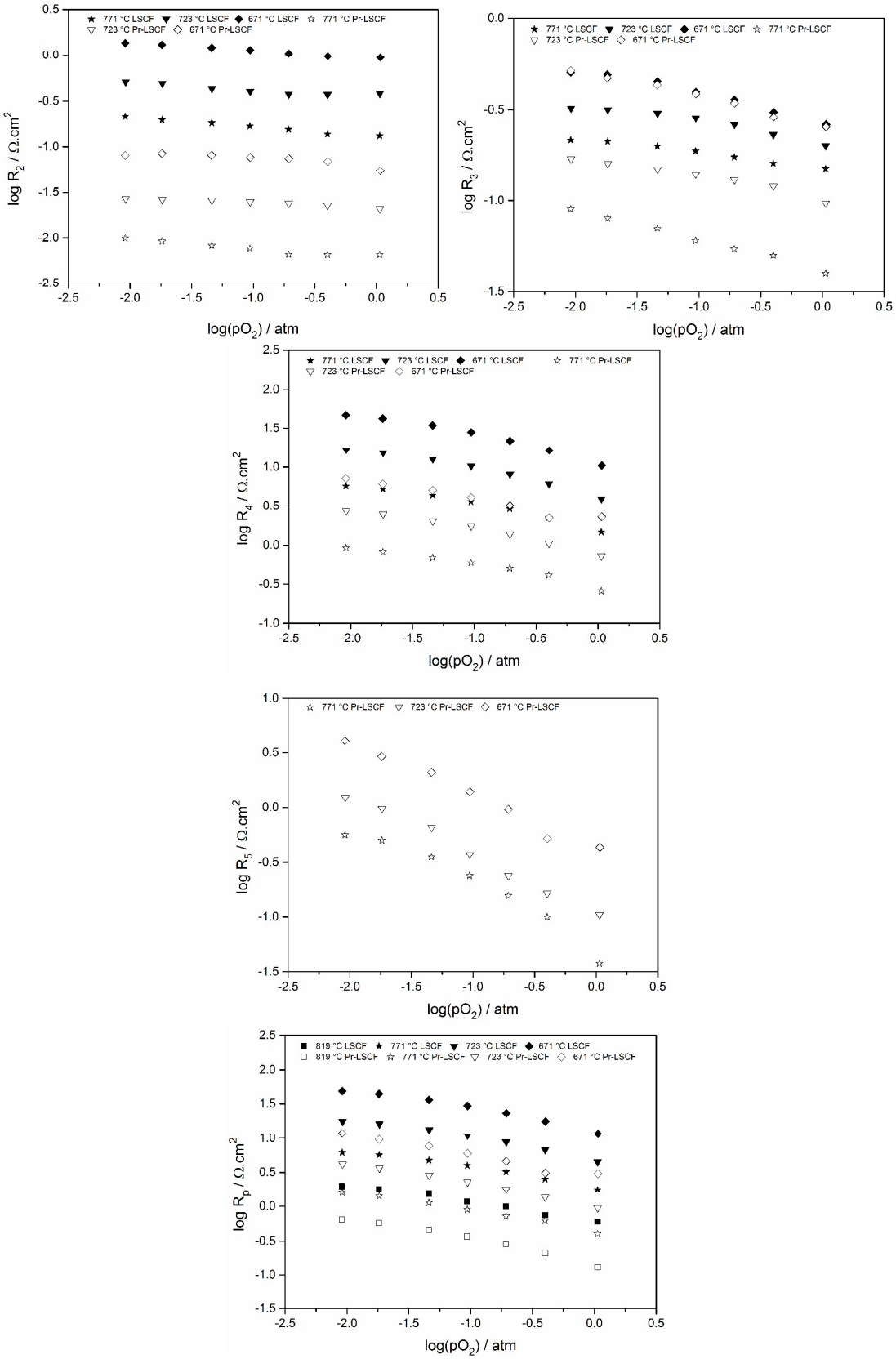

Fig. 5 – Oxygen partial pressure dependence of R_2, R_3, R_4, R_5 and R_p, in a temperature range of 671-819 °C.

Moreover, it has been outlined that the additional redox behavior of Pr^{3+}/Pr^{4+}, allows gaseous oxygen to be adsorbed as negatively charged species (O^{2-}) onto the material surface.[19] One can envisage that the ready presence of oxide-ions and their reported high storage capacity in

the $Pr_2O_2SO_4$ phase, may facilitate surface exchange processes and, hence, provide an explanation for the improvements noted in the polarization response, R_4. With respect to the polarization terms related to interfacial charge transfer, R_2, and bulk ionic diffusion, R_3, their improvement may suggest that the $Pr_2O_2SO_4$ may offer some benefit to ionic motion. Nonetheless, to date, the transport properties of this phase are unknown and are currently under study by the present authors.

The current work clearly demonstrates that the combination of the $Pr_2O_2SO_4$ phase with LSFC to form a composite cathode can significantly improve electrocatalytic performance compared to pure LSCF, predominantly due to improvements in the processes of interfacial charge transfer and surface exchange. Hence, further investigation of this material type as a candidate for use in electrode composites, for this and other systems using different MIECs, offers a highly important new avenue of SOFC cathode research.

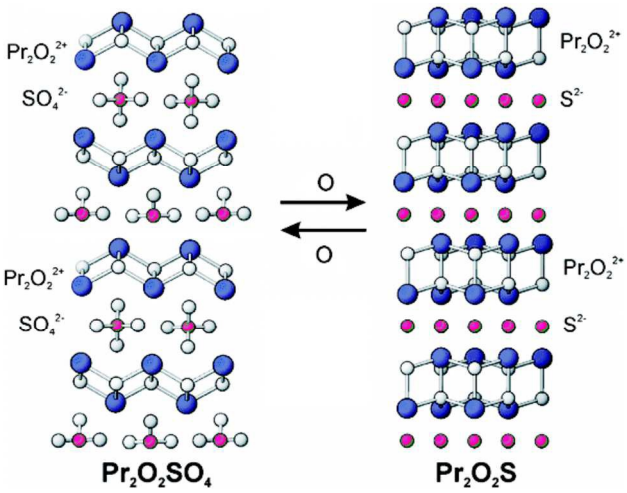

Fig. 6 – Atomic structure of the $Pr_2O_2SO_4$ and Pr_2O_2S.

Experimental section

Powders of $La_{0.6}Sr_{0.4}Co_{0.2}Fe_{0.8}O_{3-\delta}$ were prepared using the Pechini method, starting from Sigma-Aldrich chemicals of $La(NO_3)_3 \cdot 6H_2O$ (99.99 %), $Sr(NO_3)_2$ (ACS reagent, ≥ 99.0 %), $Fe(NO_3)_3 \cdot 9H_2O$ (99.99 %), $Co(NO_3)_2 \cdot 6H_2O$ (ACS reagent, ≥ 99.0 %) and citric acid (ACS reagent, ≥ 99.5 %) (metal:acid ratio was 1:5). The formed gel was heated in air at 280 °C for 2 hours and calcined further at 800 °C for 20 hours. Simultaneously, powders of $Pr_2O_2SO_4$ were prepared using a solid-state route, starting from Alfa Aesar chemicals of $Pr_2(SO_4)_3 \cdot 8H_2O$. The latter was ground in a mortar and then milled on the planetary ball mill for 6h at 500 rpm. Then, the obtained powder was heated from room temperature to 800 °C, with a dwell time of 30h, in air. The heating and cooling rates were 10 °C min^{-1}. After reaction, the aforementioned-synthesized $Pr_2O_2SO_4$ and $La_{0.6}Sr_{0.4}Co_{0.2}Fe_{0.8}O_{3-\delta}$ powders were ground in a mortar and then milled again, for 6h at 550 rpm. Powders were characterized by X-ray diffraction (Rigaku Geigerflex D/Max-C series diffractometer, using a Cu-Kα radiation).

The three-dimensional structures from LCSF and composite films were retrieved by a "slice and view" approach using a FEI Helios 450S Focused Ion Beam (FIB) - Scanning Electron Microscope (SEM). This procedure consist of sequentially etching the samples' cross-section with 30 kV Ga ions and acquiring SEM secondary-electron (SE) images using 2 kV incident electrons. The FIB etching rate and the SEM images sampling were selected to generate a 3D dataset with 10 nm cubic voxels. The thin film was covered with a 2 μm thick Pt protection layer. The SEM images post-processing and the 3D structure reconstruction were performed using the software Amira. X-ray Energy Dispersive Spectroscopy (XEDS) was performed on the same FIB-SEM microscope using 20 kV electrons.

$La_{0.6}Sr_{0.4}Co_{0.2}Fe_{0.8}O_{3-\delta}$ and $Pr_2O_2SO_4$-$La_{0.6}Sr_{0.4}Co_{0.2}Fe_{0.8}O_{3-\delta}$ (50:50 wt%, 50vol%) particle suspensions were prepared by ball-mill (PM200, Retsch, Haan, Germany) at 400 rpm for 2h followed by ultrasonic bath (Ultrasons-H, JPSELECTA, Abrera, Spain) for 1h, to break agglomerates and reduce the particle size distribution. Electrolyte disks of 1.5 mm thickness were obtained by pressing uniaxially $Ce_{0.9}Gd_{0.1}O_{2-\delta}$ powder in a 10 mm mold at 200 MPa (1 min) and heated at 1600 °C for 5h, with heating and cooling rates of 1.5 °C min^{-1}. The thin electrode films (0.264 cm^2 of effective electroactive area) were deposited over the electrolyte support by spin coating (spin coater model WS-650-23, Laurell Technologies Corporation, North Wales PA, USA) at 2000 rpm for 30s. The two symmetric cells of cathode-electrolyte assemblies were obtained by sintering in air at 1000 °C for 5h, with heating and cooling rates of 1.5 °C min^{-1}.

Electrical-conductivity measurements were performed on the symmetric cells. Platinum wire was attached to the cells in a pseudo 4-point configuration using porous Pt-paste. Impedance spectroscopy was carried out using an Electrochemie Autolab PGSTAT302N analyser in the frequency range 10^{-2}–10^6 Hz applying a signal amplitude of 50 mV. Data were collected on cooling in flowing dry O_2. The measurements were carried out using N_2-O_2 from pO_2 = 1 to 10^{-2} atm.

Acknowledgements

F. Loureiro acknowledges the project PTDC/CTM/105424/2008 funded by the Portuguese Foundation for Science and Technology (FCT) FEDER and COMPETE, with reference BI/UI66/4767/2013. Tao Yang acknowledges the FCT for financial support via the grant SFRH/BPD/86336/2012.

Author Contributions

Authors Francisco J. A. Loureiro, Tao Yang and D. P. Fagg contributed equally to this work. Daniel G. Stroppa contributed with the microstructural characterization.

Notes and references

[a] Centre of Mechanical Technology and Automation (TEMA), Department of Mechanical Engineering, University of Aveiro, 3810-193, Aveiro, Portugal.
[b] International Iberian Nanotechnology Laboratory (INL), 4715-330, Braga, Portugal.
* Corresponding author, E-mail: duncan@ua.pt; Fax: +351-234-370953; Tel: +351-234-370830.

1 J. M. Andújar, F. Segura, *Renew. Sustain. Energy Rev.*, 2009, **13**, 2309.
2 C. Bernay, M. Marchand, M. Cassir, *J. Power Sources*, 2002, **108**, 139.
3 J. H. Kim, H. Kim, *Ceram. Int.*, 2012, **38**, 4669.
4 C. Xia, M. Liu, *Adv. Mater.*, 2002, **14**, 521.
5 C. Sun, R. Hui, J. Roller, *J. Solid State Electrochem.*, 2009, **14**, 1125.
6 E. P. Murray, M. J. Sever, S. A. Barnett, *Solid State Ionics*, 2002, **148**, 27.
7 Z. Shao, S. Haile, *Nature*, 2004, **431**, 170.
8 S. Lee, H. S. Song, S. H. Hyun, J. Kim, J. Moon, *J. Power Sources*, 2010, **195**, 118.
9 W. Wang, M. Mogensen, *Solid State Ionics*, 2005, **176**, 457.
10 J. Peña-Martínez, D. Marrero-López, C. Sánchez-Bautista, A. J. dos Santos-García, J. C. Ruiz-Moralez, J. Canales-Vasquez, P. Núñez, *Bol. la Soc. Española Cerámica y Vidr.*, 2010, **49**, 15.
11 V. Dusastre, J. A. Kilner, *Solid State Ionics*, 1999, **126**, 163.
12 S. B. Adler, *Chem. Rev.*, 2004, **104**, 4791.
13 M. Liut, *J. Electrochem. Soc.*, 1998, **145**, 142.
14 D. P. Fagg, S. García-martin, V. V. Kharton, J. R. Frade, *Chem. Mater.*, 2009, **21**, 381.
15 E. V Tsipis, E. N. Naumovich, M. V Patrakeev, A. A. Yaremchenko, I. P. Marozau, A. V Kovalevsky, J. C. Waerenborgh, V. V Kharton, *Solid State Ionics*, 2011, **192**, 42.
16 D. Ramasamy, A. L. Shaula, A. Gómez-Herrero, V. V. Kharton, D. P. Fagg, *J. Memb. Sci.*, 2014, **475**, 414.
17 M. Machida, presented at *Symp. Nano-Dynamics n.d.*, Nagasaki, 2008.
18 J. Lian, X. Sun, Z. Liu, J. Yu, X. Li, *Mater. Res. Bull.*, 2009, **44**, 1822.
19 M. Machida, K. Kawamura, T. Kawano, D. Zhang, K. Ikeue, *J. Mater. Chem.*, 2006, **16**, 3084.
20 D. Marinha, L. Dessemond, E. Djurado, *J. of Power Sources*, 2012, **197**, 80.
21 V. C. Kournoutis, F. Tietz, S. Bebelis, *Fuel Cells*, 2009, **9**, 852.
22 A. Esquirol, J. Kilner, N. Brandon, *Solid State Ionics*, 2004, **175,** 63.
23 N. Grunbaum, L. Dessemond, J. Fouletier, F. Prado, L. Mogni, A. Caneiro, *Solid State Ionics*, 2009, **180**, 1448.
24. D. Waile, J. Lane, J. Kilner, B. Steele, *Solid State Ionics*, 1996, **86-88**, 767.25 Y.-M. Kim, S.-I. Pyun, J.-S. Kim, G.-J. Lee, *Jounal Electrochem. Soc.*, 2007, **154**, B802.
26 F. Baumann, J. Fleig, H-U. Habermeier, J. Maier, *Solid State Ionics*, 2006, **177**, 1071.
27 N. Simrick, A. Bieberle-Hütter, T. Ryll, J. Kilner, A. Atkinson, J. Rupp, *Solid State Ionics*, 2012, **206**, 7.

Table of contents

$Pr_2O_2SO_4$-$La_{0.6}Sr_{0.4}Co_{0.2}Fe_{0.8}O_{3-\delta}$: a new category of composite cathode for Intermediate Temperature-Solid Oxide Fuel Cells

A new category of composite cathode for solid oxide fuel cells is investigated, containing an oxysulphate oxygen storage material. A stable composite $Pr_2O_2SO_4$-$La_{0.6}Sr_{0.4}Co_{0.2}Fe_{0.8}O_{3-\delta}$ is formed, providing significant improvements in the total polarization resistance, predominantly due to improvements in the processes of interfacial charge transfer and surface exchange.

*Francisco J. A. Loureiro, Tao Yang, Daniel G. Stroppa, Duncan P. Fagg**